Transitions to Periodic Structures in Block Copolymer Melts

Monica Olvera de la Cruz

Department of Materials Science and Engineering, Northwestern University, Evanston, Illinois 60208

(Received 13 December 1990)

We study transitions to periodic structures in diblock copolymer melts including self-consistently the concentration fluctuations, and expanding the density in multiple harmonics. The fluctuations induce a shift in the maximum scattering wave vector in the isotropic state which suggests that the chains stretch near the transition. Transitions to 3D hexagonal lattices, 2D hexagonally packed cylinders, and bcc structures are predicted. We find the periodicity near the transition: The chains contract in the bcc, while they stretch in the other structures.

PACS numbers: 64.70.Dv, 05.20.−y, 36.20.Ey, 64.60.Cn

The synthesis of *A*-*B* block copolymer molecules has led to new materials with unique properties. A net repulsive interaction between the chemically linked *A* and *B* chains drives the system to segregate locally into *A*-rich and *B*-rich domains. The resulting equilibrium morphologies are periodic arrays.[1-5] Among the observed microstructures are alternating lamellae domains (lam), hexagonally packed cylinders (hpc), body-centered-cubic lattice of spheres (bcc), and bicontinuous double-diamond nets (bdd).[5]

The physical properties of an incompressible *A*-*B* block copolymer melt are strongly dependent on the degree of polymerization N, the block copolymer composition $f=N_A/N$, and the effective interaction between *A* and *B* monomers χ. When χ is small the block copolymer melt is homogeneously mixed. It undergoes a disorder-order transition (DOT) at χ_t. At the DOT the blocks segregate forming an ordered structure of periodicity d.[1-9]

Far away from the DOT in the isotropic state ($\chi\rightarrow 0$) the chains are random coils. In the ordered phases the chains are expected to be perturbed. In the weak segregation limit where the interface is large, the existing theories[6-8] assume that d scales with N^ν, $\nu=\frac{1}{2}$; i.e., the chains remain unperturbed Gaussian coils near the DOT. Experiments, however, suggest that in this limit,[1,10] and even in the isotropic state, the chains are stretched, and $\nu=0.8$, larger than in the strong segregation limit (sharp interface), where $\nu=\frac{2}{3}$.[4,9]

Including the wave-vector dependence of the vertex functions in the Hartree analysis[11,12] of the transition, we find that the concentration fluctuations induce a continuous shift in the wave vector of maximum intensity k^* as one approaches the DOT. The shift in k^* to smaller values suggests that the chains stretch in the disordered state. We calculate k^* as a function of χ and N, and the periodicity of the ordered morphology in the weak segregation regime: While in the lam and hpc the chains stretch, in the bcc they contract.

For the first time the shift in the wave vector of maximum intensity in the isotropic and ordered states is predicted using the Hartree approximation. The two-, three-, and higher-order wave-vector-dependent correlation functions in the free-energy functional of block copolymer melts allow us to calculate these effects.

In the ordered state the density in the periodic structure is expanded in multiple harmonics. The multiharmonic Hartree analysis predicts first-order transitions to 3D hexagonal close-packed structures in symmetric and nearly symmetric systems. Transitions from the isotropic state to hcp, hpc, and bcc are observed as the degree of asymmetry increases. The lam is predicted only when the transition is nearly continuous ($N>10^9$, $f\sim 0.5$ in diblocks). Our study suggests that when weakly first-order transitions to periodic structures occur, the lam is not always the equilibrium structure as was previously found.[8,11]

The free energy of the disordered state is expanded in a power series of the Fourier components of the order parameter,[6]

$$F(\rho_k)/k_BT=F_0/k_BT+(1/2!)\sum\rho_k\rho_{-k}/S_0(k)+(1/V3!)\sum\Gamma_3(k,k',k'')\rho_k\rho_{k'}\rho_{k''}\delta(k+k'+k'')$$
$$+(1/V4!)\sum\Gamma_4(k,k',k'',k''')\rho_k\rho_{k'}\rho_{k''}\rho_{k'''}\delta(k+k'+k''+k''')\,. \tag{1}$$

The order parameter $\Delta\rho(r)$ is the local deviation of $\rho(r)$, the concentration of monomer *A*, from its mean value f. The $S_0(k)$, $\Gamma_3(\{k\})$, and $\Gamma_4(\{k\})$ are functions of the bare two-, three-, and four-monomer correlation functions G_{ij}, G_{ijk}, and G_{ijkl} $(i,j,k,l=A,B)$, calculated by the random-phase-approximation method (RPA).[6,7]

In the mean-field analysis of Leibler[6] (LMFA), $S_0(k)$ is the scattering intensity in the disordered state (the RPA result):

$$1/S_0(k)=Q(x)/N-2\chi\,, \tag{2}$$

where $x=k^2Na^2/6$ and N is the number of segments of length a $(a_A=a_B)$ per chain. As $Q(x)$ has a minimum at x_0^*, $S_0(k)$ has a peak at k_0^* which is χ independent and $k_0^*(f)\sim 1/R_0\sim 1/N^{1/2}$ (R_0 is the unperturbed radius of gyration). The peak intensity $S_0(k_0^*)$ increases with χN, and for $f_c=0.5$ (when $\Gamma_3=0$) it diverges at $(\chi N)_c=Q(x_0^*(f_c))/2=10.495$.[6]

In the ordered phase $\Delta\rho(r)$ has the symmetry of the ordered structure. It is therefore expanded in a set of

TABLE I. Compositional harmonic contributions to the free energy (α_2 for the hcp is calculated using the close-packed ratio $c/a=\sqrt{8/3}$, $1/a=\sqrt{3}k^*/2$).

	n_1	n_2	α_2	$(\Gamma_3)_1$	$(\Gamma_3)_{112}$	$(\Gamma_4)_1^P$	$(\Gamma_4)_1^{\rm NP}$
lam	1	1	2	0	$-6\Gamma_3(k^*\sqrt{6/3})$	0	0
hpc	3	3	$\sqrt{3}$	$-12\Gamma_3(k^*)$	$-36\Gamma_3(k^*\sqrt{5/3})$	$12n_1[2\Gamma_4(0,1;k^*)]$	0
hcp	3	1	1.0607	$-12\Gamma_3(k^*)$	0	$12n_1[2\Gamma_4(0,1;k^*)]$	0
bcc	6	3	$\sqrt{2}$	$-48\Gamma_3(k^*)$	$-72\Gamma_3(2k^*/\sqrt{3})$	$12n_1[4\Gamma_4(0,1;k^*)+\Gamma_4(0,2;k^*)]$	$48n_1\Gamma_4(1,2;k^*)$
bdd	6	4	$\sqrt{3/2}$	$-48\Gamma_3(k^*)$	0	$12n_1[4\Gamma_4(0,1;k^*)+\Gamma_4(0,2;k^*)]$	$48n_1\Gamma_4(1,2;k^*)$
fcc	4	3	$\sqrt{4/3}$	0	$-72\Gamma_3(\sqrt{10}k^*/3)$	$12n_1[3\Gamma_4(0,4/3;k^*)]$	$12n_1[\Gamma_4(4/3,4/3;k^*)]$
Simple cubic	3	6	$\sqrt{2}$	0	$-72\Gamma_3(2k^*/\sqrt{3})$	$12n_1[2\Gamma_4(0,2;k^*)]$	0

plane waves, whose wave vectors K_i are the allowed reciprocal vectors of the ordered structure.[13] The first set of n_1 plane waves, the first harmonic, has $|K_m^{(1)}|=k^*$, $m=1,\ldots,n_1$; n_1 is the number of nearest neighbors (nn) in the reciprocal lattice, so the distance between nn planes in the structure is $d=2\pi/k^*$. The second set of plane waves has $|K_m^{(2)}|=\alpha_2 k^*$, $m=1,\ldots,n_2$; they constitute the second-order harmonic. We recently studied the LMFA for the lam, hpc, bcc, and bdd structures including harmonics up to order $|K_m^{(l)}|=3k^*$.[14] For simplicity consider only two harmonics,

$$\Delta\rho(r)=\sum_{i=1}^{2}a_i\sum_{m=1}^{n_i}\exp[i(rK_m^{(i)}+\phi_m^{(i)})]+\text{c.c.} \tag{3}$$

In the LMFA the free energy of a given morphology is obtained by replacing the wave-vector summations in (1) by sums over the allowed vectors in (3),[14] $F/k_BT=F_0/k_BT+F_1(a_1)+F_2(a_2)+F_{1,2}(a_1,a_2)$, where

$$F_i(a_i)=n_iS_0^{-1}(\alpha_ik^*)a_i^2+(\Gamma_3)_ia_i^3/3!+(\Gamma_4)_ia_i^4/4! \tag{4a}$$

($\alpha_1=1$ for all the structures and α_2 is given in Table I) and

$$F_{1,2}(a_1,a_2)=(\Gamma_3)_{112}a_1^2a_2/3!+(\Gamma_4)_{1112}a_1^3a_2/4! \\ +(\Gamma_4)_{1122}a_1^2a_2^2/4!\,. \tag{4b}$$

The $(\Gamma_3)_i$ and $(\Gamma_4)_i$ result from evaluating (1) for the ith harmonic. In the quartic term there are $6n_i$ linear arrangements $K_m^{(i)}+K_m^{(i)}-K_m^{(i)}-K_m^{(i)}=0$ denoted by $(\Gamma_4)_i^L=6n_i\Gamma_4(0,0;\alpha_ik^*)$, $12n_i(n_i-1)$ planar contributions of the form $\Gamma_4(0,h_{jm};\alpha_ik^*)$ from the arrangements $K_j^{(i)}-K_j^{(i)}-K_m^{(i)}+K_m^{(i)}=0$ with $j\neq m$ and $|K_j^{(i)}+K_m^{(i)}|^2=h_{jm}(\alpha_ik^*)^2$ denoted by $(\Gamma_4)_i^P$, and the nonplanar (NP) contributions $\Gamma_4(h_{ml},h_{mq};\alpha_ik^*)$ from the arrangements $K_m^{(i)}+K_l^{(i)}+K_j^{(i)}+K_q^{(i)}=0$ with $q\neq j\neq l\neq m$ denoted by $(\Gamma_4)_i^{\rm NP}$. Therefore, $(\Gamma_4)_i=(\Gamma_4)_i^L+(\Gamma_4)_i^P+(\Gamma_4)_i^{\rm NP}$. The terms in $F_{1,2}(a_1,a_2)$ are evaluated in a similar way.[14] The sign of $(\Gamma_3)_i$ and the mean value of a_i are determined by minimizing the free energy with respect to the phases $\{\phi_m^{(i)}\}$ and a_i.

The LMFA, however, neglects the effects of fluctuations. When the concentration fluctuations are self-consistently included in the analysis (the Hartree approximation),[11] a first-order transition is induced at f_c. This approach has been applied to block copolymers,[8,15] considering $\Gamma_3(\{k\})$ and $\Gamma_4(\{k\})$ in (1) as $\{k\}$ independent (and setting $k^*=k_0^*$, the RPA result). Here we solve the Hartree equations including the wave-vector dependence of $\Gamma_3(\{k\})$ and $\Gamma_4(\{k)\}$ in the analysis for the first time, and find the shifting of k^*. We also include higher harmonics in the Hartree analysis. In the Hartree approximation, transitions for $k^*\neq0$ are never continuous; a single set of plane waves in (3) cannot describe the density distribution in the periodic structure at the DOT. Furthermore, in the first-harmonic approximation the hpc and hcp structures cannot be distinguished, nor can the bcc and bdd.

The Hartree equations can be obtained by adding an external field $U(r)$ coupled to the order parameter in the free-energy functional (1) as $\sum U_k\rho_{-k}$, and replacing ρ_k by $g_k+\xi_k$, $F(\rho_k)=F(g_k)+G(g_k,\xi_k)$, where g_k is the mean value of the order parameter, and ξ_k are the fluctuations about it, $\langle\xi_k\rangle=0$.[12] Setting[11] $\langle\xi_k\xi_{k'}\rangle=S(k)\delta(k+k')$, $g_0=0$ (block copolymer melts are incompressible), and neglecting $\langle\xi_k\xi_{k'}\xi_{k''}\rangle$ in the relation $\langle\delta G(g_k,\xi_k)/\delta\xi_k\rangle=0$, one obtains the Hartree equation for U_{-k} and the scattering function $S(k)=\delta g_k/\delta U_k$:

$$S^{-1}(k)=S_0^{-1}(k)+H(k)/2+\Gamma_4(0,0;k)g_kg_{-k}/3+\sum_{k'\neq-k}[\Gamma_4(0,h_{kk'};|k|=|k'|)+\Gamma_4(0,h_{kk'};|k|\neq|k'|)/2]g_{k'}g_{-k'}/6\,, \tag{5}$$

where $H(k)=(2\pi)^{-3}\int\Gamma_4(0,h_{kk'};|k+k'|)S(k')d^3k'$.

Near the DOT, expanding $S^{-1}(k')$ around k^{*2} and neglecting the angular dependence of Γ_4 in the integral,[16] $H(k)=\Gamma_4(0,0;[(k^2+k^{*2})/2]^{1/2})2\alpha/\sqrt{r}$, where $\alpha=k^{*2}/4\pi c$, $c^2=x^*[\partial^2\{Q(x)+NH(k)/2\}/\partial x^2]_{x^*}/3\sim x^*[\partial^2Q/\partial x^2]_{x^*}/3$,[17] and $r=S^{-1}(k=k^*)$ is the inverse susceptibility.

The inverse susceptibility in the *disordered* state, $r_d=S_0^{-1}(k^*)+\Gamma_4(0,0;k^*)\alpha/\sqrt{r_d}$, is obtained by self-consistently finding the k^* for which $S^{-1}(k)$ is a minimum. The value of x^* vs χN is plotted in Fig. 1. The corrections in x^* from the RPA value x_0^* decrease as N increases [$x^*\sim x_0^*$ for $\chi<10^{-8}$ up to $(\chi N)\sim(\chi N)_t$], $k^*\sim k_0^*[1-O(1/N)]$.

In the ordered phase the order parameter takes the form given in (3). Evaluating U_k at $k=K_m^{(1)}$ (and neglecting the fluctuations of the second harmonic),

$$U_1=r_1a_1+\tfrac{1}{2}(\Gamma_3)_1\frac{a_1^2}{2n_1}+\tfrac{1}{6}(\Gamma_4)_1^{\mathrm{NP}}\frac{a_1^3}{2n_1}-\tfrac{1}{2}\Gamma_4(0,0;k^*)a_1^3+\frac{1}{2n_1}\frac{\partial}{\partial a_1}[F_{1,2}(a_1,a_2)-(\Gamma_4)_{1122}^{P}a_1^2a_2^2/4!]\,, \tag{6}$$

with r_1 the inverse susceptibility in the *ordered* state

$$r_1=S_0^{-1}(k^*)+\Gamma_4(0,0;k^*)\alpha/\sqrt{r_1}+B_1a_1^2+(\Gamma_4)_{1122}^{P}a_2^2/24n_1\,, \tag{7}$$

where $B_1=(\Gamma_4)_1^P/12n_1+\Gamma_4(0,0;k^*)$ and $(\Gamma_4)_{1122}^P$ are $24n_1n_2$ terms that result from the arrangements $K_j^{(1)}-K_j^{(1)}-K_m^{(2)}+K_m^{(2)}=0$ in $\Gamma_4(\{k\})$.

The free energy of the ordered phase $A(k^*)$ is given by

$$A(k^*)=\frac{n_1}{B_1}([r_1^2(k^*)-r_d^2]/2+\alpha\Gamma_4(0,0;k^*)\{[r_1(k^*)]^{1/2}-\sqrt{r_d}\})-n_1\frac{\Gamma_4(0,0;k^*)}{4}a_1^4+\frac{(\Gamma_3)_1}{3!}a_1^3$$
$$+\frac{(\Gamma_4)_1^{\mathrm{NP}}}{4!}a_1^4+F_{1,2}(a_1,a_2)-(\Gamma_4)_{1122}^{P}a_1^2a_2^2/4!+F_2(a_2)\,, \tag{8}$$

which is solved using (6) (setting $U_1=0$), (7), and $r_d(k_d^*)$, where k_d^* is the wave vector of maximum intensity in the disordered state. As near the DOT, a_2 and higher harmonics are two and higher orders of magnitude smaller than a_1 for $N>10^7$ (except for the hcp), k^* is determined by the growth of a_1. In Fig. 1 we plotted the value of x^* that minimizes $A(k^*)$ vs χN. It is common to fit the experimental data by a power law with N and χ. Though a single power law cannot describe our results, in order to compare with the experiments we found the best fit near the DOT: for the hpc and the lam $d\sim N^{\nu}$, $\nu\in[0.83,1]$, and $d\sim\chi^{\beta}$ $(\beta=\nu-\frac{1}{2})$, $\beta\in[0.335,0.5]$, close to the experimental values.[2]

In the bcc the chains contract, $\nu<\frac{1}{2}$ (Fig. 1). We have obtained k^* for other metastable structures (higher energy). In the fcc and simple-cubic structures (Table I), the chains stretch as in the hpc. In the quasicrystal with $n_1=15$ and $(\Gamma_3)_1=-120\Gamma_3(k^*)$ the chains contract as in the bcc. When α is set to zero in the Hartree equations [the LMFA (Ref. 14)], the d scaling with N for the bcc is the same as for the hpc and lam structures. Therefore, the increase in x^* with increasing N for the bcc is due to Hartree effects which appear as soon as $\alpha\neq0$. The Hartree analysis suggests that in 3D structures whose reciprocal lattice vectors form a large number of triangles the chains contract.[18]

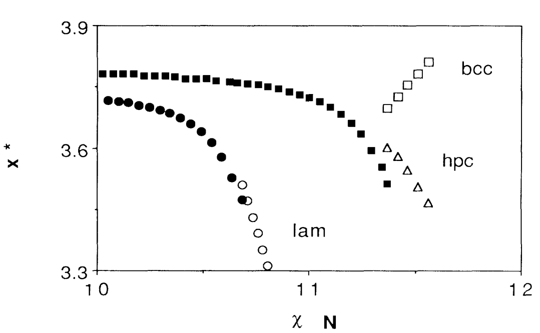

FIG. 1. $x^*=(k^*R_0)^2=k^{*2}Na^2/6$ vs χN for $f=0.6$ (upper curves), and $f=0.5$ (lower curves); $\chi=12.19\times10^{-7}$ along all the curves. The solid symbols correspond to the disordered state. In the RPA $x_0^*=3.8429$ for $f=0.6$ and $x_0^*=3.7849$ for $f=0.5$.

The higher harmonics are important to determine the equilibrium structure because the energy is very small near the DOT. If only the first harmonic is considered, the equilibrium structure for $f\in[0.5,0.5\pm\Delta]$ is the lam,[8] the structure with smallest n_1 (and the smaller the N the larger the Δ). A single-harmonic analysis, however, is valid when $N\to\infty$. For finite N, as the hcp has the smallest n_2 and a_2 values, it can be more favorable than the lam. The lam appears only when $N>10^9$ at $f\sim0.5$. For $N=10^8$ the DOT is to hcp up to $f\sim0.515$ at $(\chi N)_t\sim10.55$; as f increases, the DOT is to hpc and then to bcc [fcc is obtained for larger (χN), when the approach breaks down]. When N decreases, the width of stability of the hcp increases. The minimization in k^* and the addition of higher harmonics in (3) yield lower values of $(\chi N)_t$ than the ones obtained by a single-harmonic setting $k^*=k_0^*$; for the lam, $(\chi_t-\chi_c)\sim(\Gamma_4\alpha)^{2/3}\sim N^{-4/3}[1-O(1/N)]$. When N decreases, however, higher-order corrections need to be included in the analysis.[19]

The phases (0 or π in centrosymmetric structures) and amplitudes of higher harmonics are required to find the density distribution inside the unit cell.[14] For example, the hcp studied here is a hexagonal array of cylinders connecting lamellae layers perpendicular to the cylindrical axes, resembling a "lamellar cantenoid."

We conclude that the concentration fluctuations induce a shift in k^* in the disordered state near the DOT, and that in an ordered state the chain deformation depends on the structure. The multiharmonic Hartree approximation predicts DOT's to hcp when Γ_3 in (1) is small $(f\sim0.5)$, suggesting that the lam is not the equilibrium structure in the weak segregation regime.

I thank A. M. Mayes for the program in Ref. 15 and

for useful suggestions, M. E. Cates, B. Duplantier, C. M. Marques, and T. A. Witten for helpful discussions, and the David and Lucile Packard Foundation, the Alfred P. Sloan Foundation, and the National Science Foundation under Grant No. DMR-9057764 for financial support.

---

[1] G. Hadziioannou and A. Skoulios, Macromolecules **15**, 258 (1982); J. N. Owens, I. S. Gancarz, J. T. Koberstein, and T. P. Russell, Macromolecules **22**, 3380 (1989).

[2] T. Hashimoto, M. Shibayama, and H. Kawai, Macromolecules **13**, 1237 (1980).

[3] R. W. Richards and J. L. Thomason, Macromolecules **16**, 982 (1983).

[4] E. Helfand, Macromolecules **8**, 552 (1975).

[5] E. L. Thomas, D. M. Anderson, C. S. Henkee, and D. Hoffman, Nature (London) **334**, 598 (1988), and references therein.

[6] L. Leibler, Macromolecules **13**, 1602 (1980); A.M. Mayes and M. Olvera de la Cruz, J. Chem. Phys. **91**, 7228 (1989).

[7] M. Olvera de la Cruz and I. C. Sanchez, Macromolecules **19**, 2501 (1986).

[8] G. H. Fredrickson and E. Helfand, J. Chem. Phys. **87**, 697 (1987).

[9] A. N. Semenov, Zh. Eksp. Teor. Fiz. **88**, 1242 (1985) [Sov. Phys. JETP **61**, 733 (1985)].

[10] K. Almdal, J. H. Rosedale, F. Bates, G. D. Wignall, and G. H. Frederickson, Phys. Rev. Lett. **65**, 1112 (1990).

[11] S. A. Brazovskii, Zh. Eksp. Teor. Fiz. **68**, 175 (1975) [Sov. Phys. JETP **41**, 85 (1975)].

[12] D. J. Amit and M. Zannetti, J. Stat. Phys. **9**, 1 (1973).

[13] S. Alexander and J. McTague, Phys. Rev. Lett. **41**, 702 (1978).

[14] A. M. Mayes and M. Olvera de la Cruz (to be published).

[15] A. M. Mayes and M. Olvera de la Cruz, in *Multi-Functional Materials,* edited by E. A. Buckley, G. Gallagher-Daggitt, F. E. Karasz, and D. R. Ulrich, MRS Symposia Proceedings Vol. 175 (Materials Research Society, Pittsburgh, 1990), p. 345.

[16] The integral $H(k)$ was also done numerically yielding similar results for k^* for large N [K. Bassler and M. Olvera de la Cruz (unpublished)].

[17] $N\Gamma_4(0,0;k)$ and all $N\Gamma_3$ and $N\Gamma_4$ in Table I are linear in $x=k^2Na^2/6$ for $x\sim x_0^*$ and larger (see Ref. 14).

[18] Semenov (Ref. 9), using a completely different self-consistent approach, predicted a power-law dependence $\nu=\frac{1}{3}$, in the weak segregation regime for spherical domains regardless of the structure.

[19] J. L. Jones and M. Olvera de la Cruz (unpublished).